An integrated catalytic approach for the production of hydrogen by glycerol reforming coupled with water-gas shift

Edward L. Kunkes [a], Ricardo R. Soares [a,b], Dante A. Simonetti [a], James A. Dumesic [a,*]

[a] Department of Chemical and Biological Engineering, University of Wisconsin, 1415 Engineering Drive, Madison, WI 53706, USA
[b] Faculdade de Engenharia Química, Universidade Federal de Uberlândia, Av. João Naves de Ávila 2121, Uberlândia, MG 38408-100, Brazil

ARTICLE INFO

ABSTRACT

Reaction kinetics measurements of glycerol conversion on carbon-supported Pt-based bimetallic catalysts at temperatures from 548 to 623 K show that the addition of Ru, Re and Os to platinum significantly increases the catalyst activity for the production of synthesis gas (H_2/CO mixtures) at low temperatures (548–573 K). Based on this finding, we demonstrate a gas phase catalytic process for glycerol reforming, based on the use of two catalyst beds that can be tuned to yield hydrogen (and CO_2) or synthesis gas at 573 K and a pressure of 1 atm. The first bed consists of a carbon-supported bimetallic platinum-based catalyst to achieve conversion of glycerol to a H_2/CO gas mixture, followed by a second bed comprised of a catalyst that is effective for water-gas shift, such as 1.0% $Pt/CeO_2/ZrO_2$. This integrated catalytic system displayed ~100% carbon conversion of concentrated glycerol solutions (30–80 wt.%) into CO_2 and CO, with a hydrogen yield equal to 80% of the amount that would ideally be obtained from the stoichiometric conversion of glycerol to H_2 and CO followed by equilibrated water-gas shift with the water present in the feed.

1. Introduction

Researchers are currently developing ways to utilize renewable resources as feedstocks for energy generation and chemical production, with the aim of reducing CO_2 emissions as well as the dependency on fossil fuels. Among these efforts, hydrogen production has been attracting considerable attention. For example, hydrogen can be used as an environmentally friendly fuel and as a feedstock for ammonia-based fertilizers or other chemicals. Hydrogen is also gaining widespread applications with the advent of fuel cell technologies [1]. Additionally, many catalytic bio-fuels production processes, including several developed by our group, require a feed stream of renewable hydrogen [2–4]. In this work, we report a two-stage, single reactor process for the production of hydrogen from glycerol. Glycerol is currently produced as a by-product of the trans-esterification of fats and oils in biodiesel production [5]. Glycerol can also be produced by the fermentation of sugars [6] or catalytic hydrogenolysis of sugars and sugar-alcohols [7].

Hydrogen-rich gas mixtures can be obtained from biomass feedstocks by a two-step process. In the first step, the oxygenated organic compound generates a mixture of CO and H_2 (denoted as bio-syn-gas) according to the following Eq. (1):

$$C_nH_mO_k + (n-k)H_2O \rightarrow nCO + (n+m/2-k)H_2 \quad (1)$$
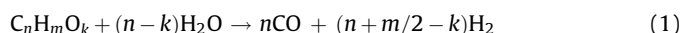
In the second step, carbon monoxide undergoes water-gas shift (WGS) with steam leading to CO_2 and the formation of additional hydrogen:

$$nCO + nH_2O \leftrightarrow nCO_2 + nH_2 \quad (2)$$

Bio-syn-gas can be produced by the gasification of carbohydrates ($n = k$) at high temperatures (800–1000 K) [8–10]. Moreover, several investigators report carrying out the overall hydrogen production process at temperatures above 873 K using glycerol as the raw material in steam reforming [11,12] or auto-thermal processes [13]. The WGS step is mildly exothermic (-40 kJ mol^{-1}), and therefore the equilibrium conversion of CO decreases at higher temperatures.

Our approach to hydrogen production outlined in this paper places emphasis on the flexibility of combining glycerol reforming with downstream WGS in one reactor system to furnish CO:H_2 mixtures with variable compositions. This flexibility allows the implementation of renewable feeds in applications that require relatively pure H_2 as well as applications requiring various grades of synthesis gas (H_2:CO = 2), such as Fischer–Tropsch synthesis and methanol synthesis [14,15]. The desired H_2:CO ratio can be achieved by changing the concentration of the carbohydrate feed (allowing water to become the limiting reagent in WGS) or

* Corresponding author. Tel.: +1 6082621095; fax: +1 6082625434.
E-mail address: dumesic@engr.wisc.edu (J.A. Dumesic).

decreasing amount of WGS catalyst, leading to incomplete conversion of CO produced in the reforming step.

To integrate the glycerol gasification and water-gas shift processes in a single reactor system, the gasification process must operate at conditions that are thermodynamically favorable for WGS (e.g., lowest temperature possible). We have previously demonstrated that carbon-supported platinum catalysts are particularly active and selective for the production of synthesis gas from glycerol at 623 K [16], because these catalysts are selective towards the cleavage of C–C bonds (leading to H_2, CO and CO_2) as opposed to C–O bonds (leading to alkanes) [17]. However, the catalyst surface becomes saturated with CO at lower temperatures, inhibiting turnover of the catalytic cycle [18]. In this respect, a catalyst with the C–O and C–C bond cleavage properties of Pt, but having a lower enthalpy of CO adsorption, would be suitable for low temperature operation.

Theoretical and experimental studies have demonstrated that the heat of CO adsorption on platinum-based catalysts can be decreased by the formation of metal alloys [19–21]. However, alloying may also alter with C–C and C–O bond cleavage characteristics, resulting in lower reforming activity and/or selectivity. Additionally, the WGS activity of the reforming catalyst must be limited, such that the extent of WGS can be controlled by the downstream catalyst. To this end, we have studied various carbon-supported, 1:1 Pt:M catalysts (M = Ru, Re, Os, Fe, Cu, Sn, Ir, Co, Ni and Rh) with respect to activity, selectivity and short-term stability for vapor phase glycerol reforming, and we have found PtRu, PtRe and PtOs to be good candidates for integration with water-gas shift.

The conditions necessary for the integration of glycerol reforming with water-gas shift place special requirements on the downstream water-gas shift catalyst. The WGS catalyst must be stable and active at intermediate temperatures, at which Cu-based WGS catalysts tend to sinter and Fe-based high-temperature WGS catalysts display low activity. Numerous investigators have observed that oxide-supported noble metal catalysts may offer significant advantages to Cu-based catalysts, including operation at higher temperatures (faster kinetics), facile activation and regeneration, stability in oxidizing conditions, and greater resistance to sintering [16,22–25]. Therefore, we have studied the WGS performance of platinum supported on a mixed cerium–zirconium oxide support at reaction conditions (e.g., H_2, CO and water concentrations) that would be found at the outlet of a glycerol reforming reactor, operating at 100% conversion of a 50 wt.% aqueous solution of glycerol at 573 K, and we have found this catalyst to be stable and active. Lastly we demonstrate that concentrated glycerol solutions (30–80 wt.%) can be processed at low temperatures (e.g., at 573 K) in a two bed-single reactor system (PtRe/C and Pt/CeZrO$_x$) to obtain 100% conversion of the carbon in glycerol to gas phase products, with a hydrogen yield equal to 80%.

2. Experimental

2.1. Catalyst preparation and characterization

Catalysts consisting of 5 wt.% Pt and 10 wt.% PtRu(1:1) supported on carbon black (Vulcan X-72C) were purchased from Etek Inc. Bimetallic PtRe, PtOs, PtFe, PtCu, PtSn, PtIr, PtCo, PtRh and PtNi, catalysts were prepared by incipient wetness impregnation of the 5 wt.% Pt Etek catalyst with aqueous solutions of $HReO_4$, H_2OsCl_6, $Fe(NO_3)_2 \cdot 9H_2O$, $Cu(NO_3)_2 \cdot 3H_2O$, $SnCl_2$, $IrCl_3 \cdot 3H_2O$, $Co(NO_3)_2 \cdot 6H_2O$, $RhCl_3 \cdot 3H_2O$, and $Ni(NO_3)_2 \cdot 6H_2O$, respectively, in sufficient concentrations to obtain 1:1 molar ratios of the metals to platinum. After impregnation, all catalysts were dried at 420 K for 12 h. All catalysts with the exception of PtSn/C, PtRe/C, and

PtOs/C were reduced at 623 K for 12 h in 200 cm^3(STP) min^{-1} flowing H_2 prior to reaction and chemisorptions measurements. PtSn/C was reduced at 573 K, and the PtOs, Re and PtRe catalysts were reduced at 723 K. The water-gas shift catalyst consisted of 1 wt.% Pt supported on CeZrO$_x$, and it was prepared according to the procedure outlined by Hori et al. [26]. In reaction kinetics studies that combined water-gas shift and glycerol reforming, both PtRe/C and Pt/CeZrO$_x$ catalysts were at reduced in 200 cm^3(STP) min^{-1} H_2 at 723 K. CO chemisorption measurements were carried out on selected catalysts to determine the metal dispersion, employing measurement of the irreversible CO uptake of the catalysts at 300 K using a standard gas adsorption apparatus described elsewhere [27].

2.2. Initial reaction kinetics studies

A 12.7 mm OD fritted-tube quartz reactor enclosed in an electrically heated furnace was used to measure the catalytic activity of bimetallic catalysts for glycerol reforming. The reactor was set up in a downflow configuration, with mass-flow controllers (Hastings) supplying hydrogen for in situ pre-treatments. The reactor wall temperature was measured with a k-type thermocouple and controlled by a PID controller (love controls) connected to a variable transformer (Tasco). An HPLC pump (Lab Alliance) was used to introduce glycerol feeds into the top of reactor, through a 6″ 5-pt needle (Hamilton). The reactor effluent was cooled to room temperature and collected in a glass separator, where the gas phase was separated and monitored with online GC analysis. A 30 wt.% glycerol solution (0.32 cm^3 min^{-1}) was fed into the reactor, containing 60–65 mg of catalyst (WHSV = 115 h^{-1}) diluted with crushed fused SiO$_2$ chips (Aldrich) to obtain a bed height of 1/2″. Whole SiO$_2$ chips (1/2″) were placed on top of the catalyst bed to aid in vaporization of the liquid feed. Measurements were taken at 623, 573 and 548 K, allowing 3 h at each temperature to achieve steady state operation. The pressure drop across the catalyst bed ranged from 0.2 to 0.4 bar. The rate of gas production was measured with a bubble meter, and the gas composition was monitored for H_2, CO, CO_2, and C_1–C_3 alkanes with TCD gas chromatography (HP 5890 TCD with helium carrier).

2.3. Detailed reaction kinetics studies

More detailed reaction kinetics studies of water-gas shift and combined glycerol conversion/water-gas shift were carried out in a reactor system similar to the one described above, except the quartz reactor was substituted with a 12.7 mm OD stainless steel tube reactor with a wall thickness of 0.71 mm. The catalyst bed was contained between an end plug of quartz wool (Alltech) and fused SiO$_2$ granules. For water-gas shift studies, 0.3 g of 1 wt.% Pt/CeZrO$_x$ was diluted with an equal volume of crushed SiO$_2$ chips and loaded into the reactor. After an in situ reduction, the reactor was brought to 573 K under flowing hydrogen, and CO (88 cm^3(STP) min^{-1}), H_2 (66 cm^3(STP) min^{-1}) and water (0.09 cm^3 min^{-1}) were fed into the reactor. This feed composition represents the mixture expected from the complete conversion of 50 wt.% glycerol (0.16 cm^3 min^{-1}) into CO and H_2. For experiments combining glycerol conversion with water-gas shift, a bed of 1 wt.% Pt/CeZrO$_x$ (1.2 g) catalyst was mixed with an equal volume of crushed SiO$_2$ granules, and this bed was loaded downstream of a glycerol conversion bed consisting of 1 g of PtRe/C diluted with an equal volume of quartz chips. After an in situ reduction, the reactor was brought to the reaction temperature under hydrogen (573 K), and the glycerol solution feed (0.04 cm^3 min^{-1}) was then introduced. Three glycerol concentrations (30%, 50% and 80%) were studied. The H_2 content of the gas phase was monitored with a Carle 8700 GC with TCD detector, and nitrogen carrier gas.
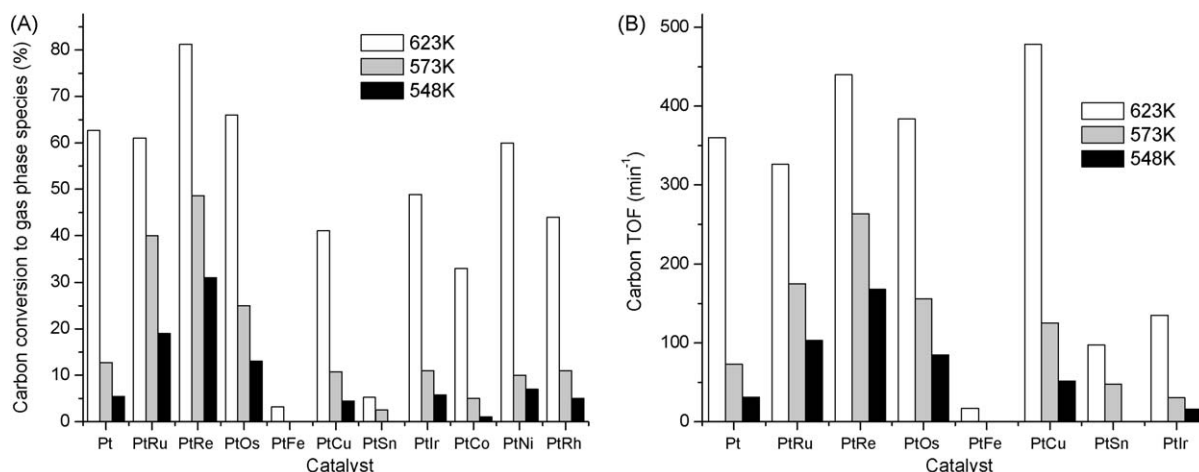
Fig. 1. (A) Glycerol conversion to gas phase over bimetallic catalysts and (B) carbon turnover frequencies for selected catalysts (30 wt.% glycerol 0.32 cm^3 min^{-1}).

3. Results and discussion

3.1. Initial studies of Pt-based bimetallic catalysts

Catalytic activities for the conversion of aqueous glycerol solutions to carbon containing gas phase products over Pt/C and platinum-based bimetallic catalysts are shown in Fig. 1A. For Pt/C, the conversion to gas phase products decreases from 63% at 623 K to 4% at 548 K. The addition of metals other that Re, Ru and Os, had a detrimental or neutral effect on catalytic activity at all reaction temperatures. The activities of PtFe/C at 573 and 548 K, and the activity of PtSn/C were too low to be quantified. It should be noted that low temperature operation is desirable for the integration of the endothermic synthesis gas production process with exothermic processes such as WGS. In this respect, the addition of Os, Ru or Re to Pt increased the production of gas phase products at the lowest temperature studied (548 K) by a factor of 2, 4 and 6, respectively, as compared to Pt/C.

The irreversible CO uptakes and dispersions for Pt/C and selected bimetallic catalysts are shown in Table 1. The addition of Fe, Cu, and Sn decreased the CO uptake, while the addition of Ir nearly doubled the original uptake as compared to Pt/C. Rioux and Vannice [28], Koerner [29] and Alcala et al. [30] observed similar effects upon the addition of Cu, Fe and Sn, respectively, to Pt catalysts. In particular, Cu and Sn do not adsorb CO significantly at room temperature and can block CO-adsorbing Pt sites. Iridium absorbs CO at room temperature, and the significant increase in CO uptake suggests that iridium forms a highly dispersed phase. The addition of rhenium does not change the CO uptake, and the addition of osmium decreases the uptake by 25%. Rhenium and osmium are known to adsorb CO at room temperature, and their effect on CO uptake suggests that Re or Os addition may increase slightly the average particle size of the metallic phase. Ni and Co absorb CO at room temperature, but have been observed to possess

low dispersions when supported on carbon [31,32], and it is likely that these metals block CO adoption sites in manner similar to that of Cu, Fe and Sn.

Fig. 1B shows the activity of various represented catalysts as carbon turnover frequencies (TOF). This quantity is the molar rate of carbon production in the gas phase products normalized by the number of surface sites for CO adsorption, the latter measured at 300 K. At 548 K, the PtRu/C, PtRe/C, and PtOs/C catalysts are 3, 5 and 3 times more active than Pt/C, respectively. The PtCu/C catalyst displayed the highest normalized (TOF) activity at 673 K, indicating a possible promotional effect of Cu. However, this promotional effect is much less apparent at lower reaction temperatures. The addition of iridium and rhodium did not significantly reduce activity with respect to conversion, whereas a negative effect of Ir addition on the TOF was observed. This effect may be caused by CO poisoning of Ir sites, due to the high binding energy of CO on Ir (−2.12 eV) as compared to Pt (−1.8 eV) [33].

We have previously demonstrated the absence of mass transfer limitations for the vapor phase reforming of a 30 wt.% glycerol solution on a similar Vulcan X-72C-supported PtRe catalyst at the conditions used in this work [34]. Additionally we have shown that the Weisz–Prater criterion for intra-particle mass transfer limitations [35] is satisfied, ensuring that the turnover frequencies reported in this work are free from transport artifacts.

Arrhenius representations of the rate data for Pt, PtRu, PtRe and PtCu catalysts are shown in Fig. 2. The apparent activation energies calculated from Fig. 2 are 93, 84, 43 and 35 kJ mol^{-1} for Pt, PtCu, PtRu, and PtRe, respectively. The lower apparent activation energies observed for PtRe and PtRu lead to enhanced activity at low reaction temperatures. It has been shown previously that strong adsorption of CO on the catalyst surface has a negative effect on the aqueous phase reforming reaction of ethylene glycol to yield hydrogen and CO$_2$ [36]. Experimental and theoretical studies have shown that addition of Ru and Re to platinum decreases the binding energy of CO on the surface, thereby leading to faster turnover of catalytic sites [19,33,37]. Promotional effects of Ru, Re and Os are particularly evident at low temperatures, where CO coverages on Pt are expected to be high [18].

Fig. 3A shows the H$_2$/CO ratio for various catalysts at different temperatures. The value of this ratio ranged from 1.2 to 1.3 for all catalysts, except for PtFe and PtSn, PtCu, PtCo and PtNi at 573 and 548 K, and PtRe at 623 K. This range of values is in agreement with the CO/H$_2$ ratio of 1.33 resulting from the stoichiometric conversion of glycerol into CO and H$_2$. The high H$_2$/CO ratio observed for PtRe, PtFe and PtSn results from enhanced rates of water-gas shift on these catalysts, in agreement with reports that

Table 1
CO chemisorption properties of selected catalysts.

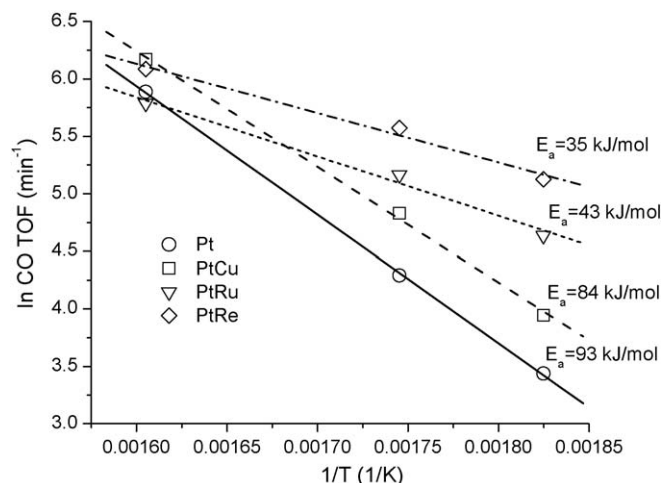| Catalyst	Sites (μmol g^{-1})	CO/M	CO/Pt
Pt	107	0.42	0.42
PtRe	107	0.26	0.53
PtRu	90	0.13	0.27
PtOs	82	0.16	0.32
PtFe	50	0.10	0.20
PtCu	50	0.10	0.20
PtSn	58	0.11	0.23
PtIr	213	0.42	0.83

Fig. 2. Arrhenius plot and activation energies for CO production from glycerol for selected bimetallic catalysts.

Re, Fe-oxides and Sn function as WGS promoters for Pt [25,38]. For PtCu, PtCo and PtNi catalysts, the H_2/CO ratio appears to decrease with increasing reaction temperature. This behavior may result from dehydrogenation of glycerol at lower temperatures to yield carbonyl products such as acetol, di-hydroxy acetone and glyceraldehyde. This dehydrogenation is not accompanied by C–C bond cleavage and therefore yields H_2 without releasing CO or CO_2. At higher temperature, the rate of C–C cleavage increases and the H_2/CO ratio approaches the stoichiometric ratio of 1.33. A similar trend in hydrogen production was observed by Zhang et al. for the steam reforming of ethanol over Co- and Ni-based catalysts [39].

3.2. Glycerol conversion combined with water-gas shift

To achieve the maximum hydrogen yield from glycerol conversion, it is necessary to couple synthesis gas production with water-gas shift. To accomplish this coupling, process conditions that allow the complete conversion of glycerol to CO and H_2 and the maximum conversion of CO via WGS are required. Previous work from our group [16] indicates that it is possible to convert nearly 80% of the glycerol in a 30 wt.% glycerol solution to H_2:CO gas mixtures when carrying out the reaction over a PtRu/C catalyst at space velocities lower than $3\,h^{-1}$ at atmospheric pressure and 573 K. At similar space velocities and 498 K, a
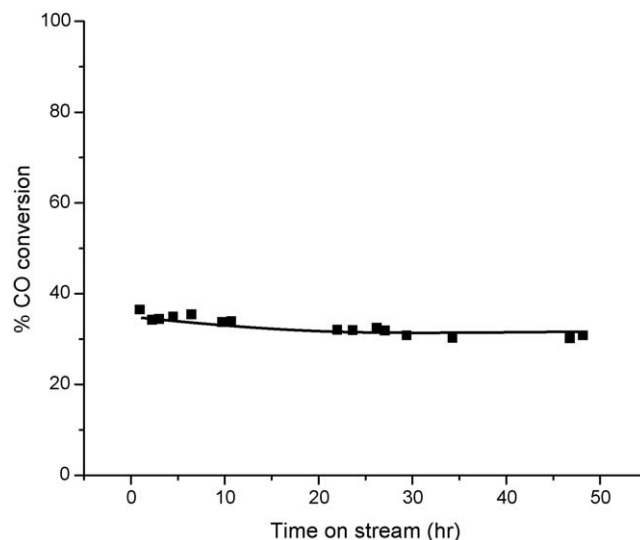

Fig. 4. Performance versus time on stream of 1 wt.% $Pt/CeZrO_x$ catalyst at CO, H_2 and H_2O flow rates equivalent to 100% conversion of 50 wt.% glycerol solution ($0.16\,cm^3\,min^{-1}$) into H_2/CO mixtures.

conversion of 40% was achieved over PtRe/C. To ensure near complete conversion of glycerol to synthesis gas, we operated our dual-bed system at significantly lower space velocities of $0.8–2\,h^{-1}$ (calculated with respect to the glycerol reforming catalyst) at 573 K, using the best reforming catalyst (PtRe) found in our initial studies.

The performance and stability of the water-gas shift catalyst are shown in Fig. 4. The 1.0% $Pt/CeO_2/ZrO_2$ catalyst, operating at a space velocity of $18\,h^{-1}$, converts 36% of the CO contained in a feed mixture representing that obtained from complete conversion of a 50 wt.% glycerol solution. To ensure near equilibrium conversion of the CO produced from glycerol reforming, the dual-bed system was operated at space velocities of $0.7–1.6\,h^{-1}$ (calculated with respect to the $Pt/CeZrO_x$ weight). Fig. 5 shows the performance of the two-bed system (Pt–Re/C followed by $Pt/CeZrO_x$) in processing 30 and 80 wt.% solutions of glycerol in water at 573 K and atmospheric pressure. The system exhibited excellent stability during the 48 h time-on-stream and the H_2/CO ratio obtained varied significantly with the glycerol content. At the highest glycerol concentration, the value was close to 2.0, which is appropriate for methanol or Fischer–Tropsch syntheses. For a feed containing 30 wt.% glycerol, we observed a product gas stream with a low CO concentration
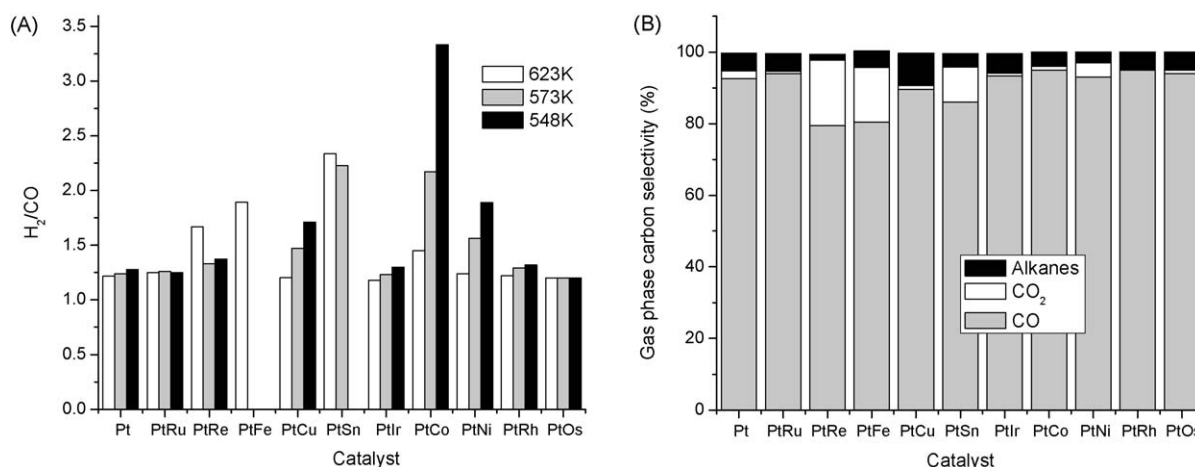

Fig. 3. (A) H_2/CO ratio in the gas phase and (B) Gas phase carbon distributions for glycerol reforming and (30 wt.% glycerol, $0.32\,cm^3\,min^{-1}$ at 623 K).
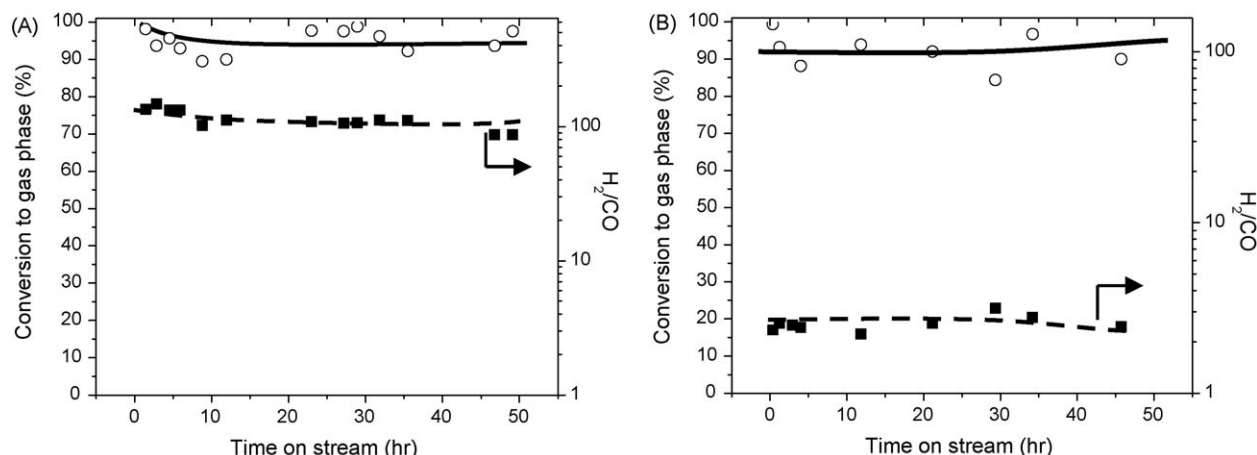
Fig. 5. Performance of stacked bed glycerol reforming (PtRe/C) and water-gas shift (PtCeZrO$_x$) system at 573 K and 0.04 cm^3 min^{-1} glycerol (A) 30 wt.% and (B) 80 wt.%.

(5000 ppm). Thus, we find that conversion of glycerol to gas products having a low CO content is favored with dilute glycerol feeds. In this respect, the presence of excess water favors the conversion of CO reaction to H$_2$ and CO$_2$ via WGS.

It is noteworthy that we obtain turnover frequencies for CO production near 85–160 min^{-1} at 523 K on the most active catalysts (PtRe, PtRu and PtOs), while operating at 10–30% glycerol conversion. If this CO is converted to equilibrium via water-gas shift, then the resulting turnover frequency for H$_2$ production would be in the range of 150–250 min^{-1}, a value that is an order of magnitude higher than the rate of H$_2$ production at similar conditions by aqueous phase reforming ($\sim$10 min^{-1}) [40]. This results suggests that gas phase reforming may be a better alternative for hydrogen production than aqueous phase reforming for high concentrations of glycerol.

Table 2 summarizes glycerol reforming results obtained after 40 h time-on-stream with different glycerol contents at 573 K, using PtRe/C, followed by Pt/CeZrO$_x$. To quantify the efficiency of hydrogen production, we have calculated the maximum hydrogen yield, which is obtained after the stoichiometric conversion of glycerol into CO and H$_2$, followed by the equilibrated water-gas shift of the CO with water present in the feed (Table 2). For all glycerol concentrations, the hydrogen yield approached 80% of this calculated maximum. We have also calculated the H$_2$/CO ratios resulting from equilibrated water-gas shift, and we have observed that the reaction effluents possess H$_2$/CO ratios similar to those obtained from WGS equilibrium, indicating that WGS is, in fact, near equilibrium. We also note that the selectivity to alkanes increases with glycerol concentration, and results from C–O cleavage side reactions, which are favored at high coverages of the catalyst surface by species derived from oxygenated intermediates [17].

To examine the viability of the dual-bed system we must consider the loss in energy efficiency associated with the

processing of dilute feedstocks, resulting from water vaporization and the reduction in the H$_2$ content of the effluent while processing more concentrated feedstocks. If we subtract the energies used for vaporizing and heating the aqueous feed solution, and operating the endothermic glycerol conversion reaction from the heat released by the combustion of the reaction products (lower heating values of CO and H$_2$), then we obtain the net energy content of the gas stream produced by the process. This value becomes positive at glycerol concentrations higher than 17 wt.% at 573 K, as shown in Fig. 6. Assuming the WGS reaction is equilibrated, the maximum efficiency for direct hydrogen production occurs at concentration around 60 wt.%, reaching a net gain of 1100 kJ mol^{-1} of glycerol processed. Above this value, this gain diminishes due to decreasing CO conversion by WGS. If we consider the utilization of CO, then the energy gain increases monotonically as a function of glycerol concentration; however, the differential gain in energy diminishes with increasing glycerol concentration.

It is noteworthy that the value of the glycerol concentration leading to zero input of energy does not change significantly when the reaction temperature changed by 50 K, since the energy required to heat the feed to the reaction temperature is small compared to the heat of vaporization. Nonetheless, the ability of performing the reaction at lower temperature brings the benefit of utilizing lower grade heat sources, and implementing heat recycling from other processes.
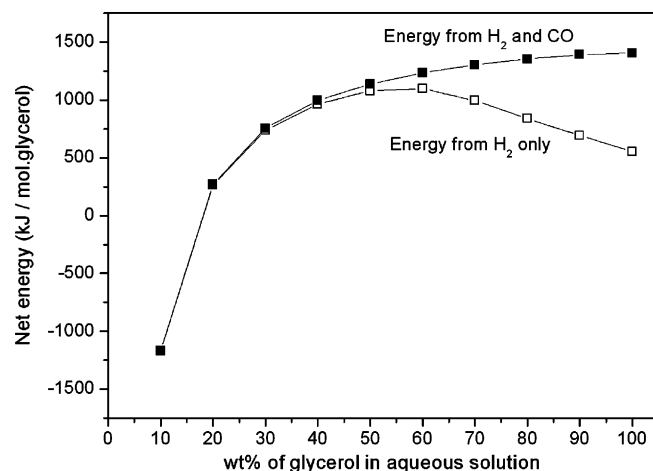
Table 2

Hydrogen production from glycerol reforming in stacked bed system (PtRe/C and Pt/CeZrO$_x$) at 573 K and 0.04 cm^3 min^{-1} glycerol flow rate.

	Glycerol (wt.%)		
	30	50	80
Carbon conversion	95%	100%	94%
Alkane selectivity	4%	5%	8%
H$_2$/CO (measured)	97	27	2.6
H$_2$/CO (predicted)	118	32	2.9
H$_2$ yield	80%	79%	78%

Fig. 6. Net energy balance for glycerol reforming into H$_2$/CO mixtures, coupled with water-gas shift at 573 K.

4. Conclusions

An integrated catalytic system to produce synthesis gas with controlled H_2:CO ratios can be fashioned using two catalyst beds. The first bed consists of a PtRe/C catalyst to achieve high conversions of glycerol to produce a H_2/CO gas mixture, followed by a second bed containing a thermally stable and active water-gas shift catalyst, such as 1.0% $Pt/CeO_2/ZrO_2$. This two-bed, single reactor system serves as an energy-efficient approach to produce hydrogen from biomass-derived feedstocks.

Acknowledgements

References

[1] Kirk-Othmer Encyclopedia of Chemical Technology, John Wiley & Sons, New York, 2001.
[2] R.M. West, Z.Y. Liu, M. Peter, J.A. Dumesic, Chem. Sus. Chem. 1 (2008) 417.
[3] G.W. Huber, R.D. Cortright, J.A. Dumesic, Angew. Chem. Int. Ed. 43 (2004) 1549–1551.
[4] M.A. Dasari, P.-P. Kiatsimkul, W.R. Sutterlin, G.J. Suppes, Appl. Catal. A 281 (2005) 225–231.
[5] D.L. Klass, Biomass for Renewable Energy, Fuels, and Chemicals, Academic Press, San Diego, 1998.
[6] C.S. Gong, J.X. Du, N.J. Cao, G.T. Tsao, Appl. Biochem. Biotechnol. 84–86 (2000) 543–559.
[7] T. Werpy, Hydrogenolysis of 6-carbon sugars and other organic compounds, EU C07C29/00.
[8] M. Asadullah, S. Ito, K. Kunimori, M. Yamada, K. Tomishige, Environ. Sci. Technol. 36 (2002) 4476–4481.
[9] P.L. Spath, D.C. Dayton, Preliminary Screening—Technical and Economic Assessment of Synthesis Gas to Fuels and Chemicals with Emphasis on the Potential for Biomass-Derived Syngas, National Renewable Energy Laboratory, Golden, CO, 2003.
[10] R.L. Bain, D.C. Dayton, D.L. Carpenter, S.R. Czernik, C.J. Feik, R.J. French, K.A. Magrini-Bair, S.D. Phillips, Ind. Eng. Chem. Res. 44 (2005) 7945–7956.
[11] S. Adhikari, S. Fernando, A. Haryanto, Catal. Today 129 (2007) 355–364.
[12] T. Hirai, N. Ikenaga, T. Miyake, T. Suzuki, Energy Fuels 19 (2005) 1761–1762.
[13] P.J. Dauenhauer, J.R. Salge, L.D. Schmidt, J. Catal. 244 (2006) 238–247.
[14] K.A. Pokrovski, M.D. Rhodes, A.T. Bell, J. Catal. 235 (2005) 368.
[15] E. Iglesia, S.C. Reyes, R.J. Madon, S.L. Soled, Adv. Catal. 39 (1993) 221.
[16] R.R. Soares, D.A. Simonetti, J.A. Dumesic, Angew. Chem. Int. Ed. 45 (2006) 3982–3985.
[17] R. Alcala, M. Mavrikakis, J.A. Dumesic, J. Catal. 218 (2003) 178–190.
[18] R. He, R.R. Davda, J.A. Dumesic, J. Phys. Chem. B 109 (2005) 2810–2820.
[19] Y. Ishikawa, M.S. Liao, C.R. Cabrera, Surf. Sci. 513 (2002) 98–110.
[20] J. Greeley, M. Mavrikakis, Nat. Mater. 3 (2004) 810–815.
[21] E. Christoffersen, P. Liu, A. Ruban, H.L. Skriver, J.K. Norskov, J. Catal. 199 (2001) 121–131.
[22] P. Panagiotopoulou, D.I. Kondarides, J. Catal. 225 (2004) 327–336.
[23] R.J. Gorte, S. Zhao, Catal. Today 104 (2005) 18–24.
[24] T. Bunluesin, R.J. Gorte, G.W. Graham, Appl. Catal. B 15 (1998) 107–114.
[25] Y. Sato, K. Terada, S. Hasegawa, T. Miyao, S. Naito, Appl. Catal. A 296 (2005) 80–89.
[26] C.E. Hori, H. Permana, K.Y.S. Ng, A. Brenner, K. More, K.M. Rahmoeller, D. Belton, Appl. Catal. B 16 (1998) 105–117.
[27] B.E. Spiewak, J. Shen, J.A. Dumesic, J. Phys. Chem. 99 (1995) 17640.
[28] R.M. Rioux, M.A. Vannice, J. Catal. 233 (2005) 147.
[29] L. Koerner, Chemical and Biological Engineering, University of Wiscnonsin-Madison, Madison, 2004.
[30] R. Alcala, J.W. Shabaker, G.W. Huber, M.A. Sanchez-Castillo, J.A. Dumesic, J. Phys. Chem. B 109 (2005) 2074–2085.
[31] S. Yao, C. Yang, Y. Tan, Y. Han, Catal. Commun. 9 (2008) 2107–2111.
[32] G.L. Bezemer, P.B. Radstake, U. Falke, H. Oosterbeek, H.P.C.E. Kuipers, A. van Dillen, K.P. de Jong, J. Catal. 237 (2006) 152–161.
[33] J. Greeley, M. Mavrikakis, Catal. Today 111 (2005) 52–58.
[34] D.A. Simonetti, E.L. Kunkes, J.A. Dumesic, J. Catal. 247 (2007) 298–306.
[35] M.A. Vannice, Kinetics of Catalytic Reactions, Springer, New York, 2005.
[36] J.W. Shabaker, R.R. Davda, G.W. Huber, R.D. Cortright, J.A. Dumesic, J. Catal. 215 (2003).
[37] A. Ramstad, B. Strisland, S. Raaen, A. Borg, C. Berg, Surf. Sci. 440 (1999) 290–300.
[38] X. Wang, R.J. Gorte, Appl. Catal. A (2003) 157.
[39] B. Zhang, X. Tang, Y. Li, Y. Xu, W. Shen, Int. J. Hydrogen Energy 32 (2007) 2367–2373.
[40] R.R. Davda, J.W. Shabaker, G.W. Huber, R.D. Cortright, J.A. Dumesic, Appl. Catal. B 43 (2003) 13–26.